Time domain surface impedance concept for low frequency electromagnetic problems—Part II: Application to transient skin and proximity effect problems in cylindrical conductors

S. Barmada, L. Di Rienzo, N. Ida and S. Yuferev

Abstract: A time domain boundary element formulation employing the surface impedance boundary conditions (SIBCs) is developed for the 3-dimensional transient eddy current problem of cylindrical conductors. SIBCs of different orders of approximation are implemented using the perturbation technique in the small parameter proportional to the ratio of the skin depth and characteristic size of the conductor cross-section. The formulation consists of a set of time domain surface integral equations that have identical left-hand sides and can be solved using the same program procedure. The number of equations is determined by the order of approximation of the SIBC, namely: solutions in the perfect electrical conductor (PEC) limit (lowest order) and in the so-called Rytov approximation (highest order) are given by one and four equations, respectively. It is demonstrated that each equation admits separation of variables into space and time components, a property that significantly reduces computational costs compared with traditional time domain formulations that require the integral equations to be solved at each time step. For the purpose of validation, a test problem is solved by the proposed formulation and by the 'original' BEM based on the time-dependent fundamental solution. Conditions of applicability are discussed and the effect of such factors as the shape of the incident current pulse and proximity effect are considered.

1 Introduction

In Part I of this two part paper [1] we developed surface impedance boundary conditions in the time- and frequency-domain on the smooth curved surface of a homogeneous conductor. Scale factors for the basic variables were introduced with the end result that a small parameter, equal to the ratio of the depth of penetration and the body's characteristic size, appears in the dimensionless Maxwell's equations for the conducting region. This fact is then exploited using perturbation techniques to represent the SIBCs in the form of power series in this small parameter. The first term (zeroth order term) of the expansion was shown to be the solution in the perfect electric conductor (PEC) limit which does not allow penetration of electromagnetic fields into the conductor. The second term (first-order term) was shown to be the solution of the problem in the Leontovich approximation, which allows penetration and diffusion into the conductor perpendicular to the interface. The interface itself is planar and the fields do not vary on the interface. The third term (second-order term) was shown to be the solution in the Mitzner approximation. In this approximation the curvature of the body is taken into account but the diffusion is again normal to the interface and no variation of the fields on the interface is allowed. The third-order term and higher allow for diffusion of fields in tangential and normal directions on curved interfaces. This was referred to as the Rytov approximation.

For completeness, and to set the stage for the formulation and results that follow, we summarise here the main results together with the assumptions used to obtain them as described in Part I of this paper. For the sake of brevity, only those relations referred to in this part are given explicitly. For the derivation of these relations the reader is referred to [1].

First and foremost we have assumed that the time variation of the incident field is such that the skin depth δ remains small compared with the characteristic dimension D of the body's surface

$$\delta = \sqrt{\tau/\sigma\mu_1} \ll D \tag{1}$$

where τ is the ratio $2/\omega$ in the case of time-harmonic fields or the incident pulse duration in the case of transient sources, σ and μ_1 are the conductivity and permeability of the conducting medium, and D is taken as the minimum radius of curvature on the surfaces of the conducting media. Displacement currents are neglected. Further, it is assumed that the conducting body is surrounded by a non-conducting medium, that the source of the field is in this medium outside the conductors and all media are homogeneous. A system of local coordinates is used whereby ξ_1 and ξ_2 are tangential to the surface of the conductor and η is perpendicular and pointing into the conductor.

IEE Proceedings online no. 20049036

doi:10.1049/ip-smt:20049036

Paper first received 25th February 2004 and in revised form 1st February 2005

S. Barmada is with the Università di Pisa, Via Diotisalvi 2, Pisa 56126, Italy

L. Di Rienzo is with the Politecnico di Milano, P.za L. Da Vinci 32, Milano 20133, Italy

N. Ida is with the ECE. Dept., University of Akron, Akron OH 44325-3904, USA

S. Yuferev is with the Nokia Corporation, P.O.Box 1000, Tampere FIN-33721, Finland

E-mail: ida@uakron.edu

The condition in (1) allows us to transform Maxwell's equations by using asymptotic expansion techniques from which we derived the normal components of the magnetic field and the tangential components of the electric field at the body's surface in explicit form. To do so we introduce characteristic scale factors for the variables of the problem. The characteristic size D is used as a scale for the surface coordinates ξ_1 and ξ_2 whereas for the coordinate η we use the skin depth δ. Additional scale factors are needed for the field variables. With these scale factors, the following non-dimensional variables are obtained:

$$\tilde{\xi}_k = \xi_k/D; \quad \tilde{t} = t/\tau; \quad \tilde{\eta} = \eta/\delta; \quad \tilde{E} = E/E^*; \quad \tilde{H} = H/H^* \tag{2}$$

where H^* and E^* are the scale factors for the electric and magnetic field, respectively. It is further shown in [1] that these two scale factors are not independent and may be expressed in terms of a single scale factor, which in many cases may be chosen as the total input current I^* but, in general, the scale factor is based on the inputs of the problem to be solved. In all, only three independent scale factors are required. If we choose I^* as the scale factor for fields, we have from the Biot-Savart law:

$$H^* = I^*/(4\pi D^*) \tag{3}$$

The scale factor may be similarly expressed in terms of I^* directly from Maxwell's equations in non-dimensional form.

From (1) and (2) we can write the following:

$$\delta = \sqrt{\tau/(\sigma\mu_1)} = \sqrt{\tau/(\sigma\mu_1 D^2)}D = pD; \quad p = \delta/D = \sqrt{\tau/(\sigma\mu_1 D^2)} \ll 1 \tag{4}$$

where the parameter p is clearly small and is proportional to the ratio of the skin depth and the characteristic size of the conductor's surface.

With these assumptions and definitions we then proceed to write the time-dependent Maxwell's equations in non-dimensional form and transform them into the Laplace domain to eliminate explicit time dependency. Then, we represent the variables for which solutions are sought in the form of asymptotic expansions in the small parameter p. The terms of these expansions then provide the various order SIBCs in the Laplace domain. We specifically identify the zeroth-, first-, second- and third-order expansions as the PEC, Leontovich, Mitzner and Rytov surface impedance boundary conditions respectively.

Applying the inverse Laplace transform provides the time domain SIBCs in non-dimensional variables. Finally, returning to dimensional variables we obtain the SIBCs of the various orders. These are:

$$E^b_{\xi_k} = (-1)^{3-k}\left\{\hat{T}_1 * H^b_{\xi_{3-k}} + \frac{d_k - d_{3-k}}{2d_k d_{3-k}}\hat{T}_2 * H^b_{\xi_{3-k}} + \frac{3d_k^2 - d_{3-k}^2 - 2d_k d_{3-k}}{8d_k^2 d_{3-k}^2}\hat{T}_3 * H^b_{\xi_{3-k}} + \frac{\hat{T}_3}{2} * \left(-\frac{\partial^2 H^b_{\xi_{3-k}}}{\partial \xi_k^2} + \frac{\partial^2 H^b_{\xi_{3-k}}}{\partial \xi_{3-k}^2} + 2\frac{\partial^2 H^b_{\xi_k}}{\partial \xi_k \partial \xi_{3-k}}\right)\right\} + \ldots \quad k = 1, 2 \tag{5a}$$

$$H^b_\eta = \sum_{i=1}^{2}\frac{\partial}{\partial \xi_i}\left\{T_1 * H^b_{\xi_i} + \frac{d_{3-1} - d_1}{2d_i d_{3-i}}T_2 * H^b_{\xi_i} + \frac{3d_{3-i}^2 - d_i^2 - 2d_i d_{3-i}}{8d_i^2 d_{3-i}^2}T_3 * H^b_{\xi_i} + \frac{T_3}{2} * \left(-\frac{\partial^2 H^b_{\xi_i}}{\partial \xi_{3-i}^2} + \frac{\partial^2 H^b_{\xi_i}}{\partial \xi_i^2} + 2\frac{\partial^2 H^b_{\xi_{3-i}}}{\partial \xi_i \partial \xi_{3-i}}\right)\right\} + \ldots \tag{5b}$$

where the sign '$*$' denotes a time convolution product. In these relations

$$T_1(t) = (\pi\sigma\mu_1)^{-1/2}t^{-1/2}; \quad T_2(t) = U(t)/(\sigma\mu_1); \quad T_3(t) = 2\left(\pi\sigma^3\mu^3\right)^{-1/2}t^{1/2}; \quad \hat{T}_1(t) = -(4\pi\sigma/\mu_1)^{-1/2}t^{-3/2}; \quad \hat{T}_2(t) = U^2(t)/\sigma; \text{ and } \hat{T}_3(t) = \left(\pi\sigma^3\mu_1\right)^{-1/2}t^{-1/2}. \tag{5c}$$

The time domain surface impedance boundary conditions in (5) include the first four terms of the expansion (that is, they represent the Rytov SIBCs). Lower order SIBCs may be obtained by neglecting the appropriate terms in the expansions. These SIBCs will now be employed for solution of skin and proximity effect problems in cylindrical conductors for the purpose of comparing the accuracy of the various order SIBCs.

The numerical method best suited for use with surface impedance boundary conditions is the boundary element method because in BEM and SIBC the functions are approximated at the same points on the interface between the media. Being applied to an eddy current problem consisting of conducting and non-conducting regions, the boundary element method yields a system of two integral equations over the conductor's surface with respect to two unknowns: the required function and its normal derivative at the conductor/dielectric interface [2]. Under the conditions of the skin effect, the electromagnetic field behaviour in the conductor is known, the surface impedance concept may be applied and the formulation can be reduced to a single integral equation employing the fundamental solution of the Laplace equation. The extra unknown is eliminated using the surface impedance boundary condition(s) relating the function and its normal derivative at the conductor's surface. This approach is almost ideal for solution of time harmonic problems and BEM-SIBC formulations have been widely used for analysis of skin and proximity effect problems of multiconductor systems [3–9].

In the general case of transient excitation, the surface integral equation including the time domain SIBC in the form (5) has to be solved at every time step due to the time convolution terms. It leads to a significant increase in the computational cost required for solution and for all practical purposes renders impractical its numerical implementation. The best way to avoid this difficulty is separation of variables in the formulation into space and time components. In this case the integral equation for the space component needs to be solved only once for a given system of conductors and the result multiplied by the time component to obtain the solution of the problem for any time dependence of the source.

It is easy to see that the variables in (5) cannot be separated because the functions T_m are different. However, each term in (5) being considered independently admits separations of variables. This circumstance and the fact that the SIBC in (5) can be represented as power series in the

small parameter are keys to the development of the desired formulation. Indeed, it is natural to suppose that use of the perturbation technique, as described in Part I of this work, will lead to a set of integral equations so that every equation includes only one term of (5) and, consequently, admits separation of variables. Such a formulation has clear physical meaning: the zero-order integral equation gives the solution in the well-known perfect electrical conductor limit and other equations yield corrections of the order of Leontovich's, Mitzner's and Rytov's approximations. Thus the total number of integral equations in the formulation will not exceed four. In fact, it may be even less depending on the problem [10]. Derivation of such a formulation is the first aim of this work.

Another goal is numerical validation of the formulations employing time domain surface impedance boundary conditions to clarify the limits of applicability of the concept. This problem has been already considered in the past [11–13] but the reported works focused on the classical single-frequency SIBC. Investigation of the impact of such factors as shape of the incident pulse and the proximity effect on the approximation error of the time domain BEM-SIBC formulations is another aim of the work.

2 Statement of the problem and basic equations

Consider a system of N cylindrical conductors of arbitrary cross-sections surrounded by homogeneous non-conducting space as shown in Fig. 1. The parameters of the conducting and non-conducting media are assumed to be constants. Let an external source produce quasi-steady current pulses flowing through the conductors so that

$$\vec{I}_i(\vec{r},t) = \vec{I}_i^{sp}(\vec{r})\tilde{\theta}_0(t), \quad \oint_{C_i} \vec{H}\cdot d\vec{l} = I_i \quad i = 1,2\ldots N \tag{6}$$

where $\tilde{\theta}_0$ is a known non-dimensional time dependent function that is the same for all conductors, $\vec{I}_i^{sp}$, $i = 1,2\ldots N$, are vectors setting the magnitude and direction of the total current flowing in the conductor and C_i is an arbitrary path enclosing the ith conductor. Let the duration of the pulse be such that the skin layer is thin and condition (1) is met.

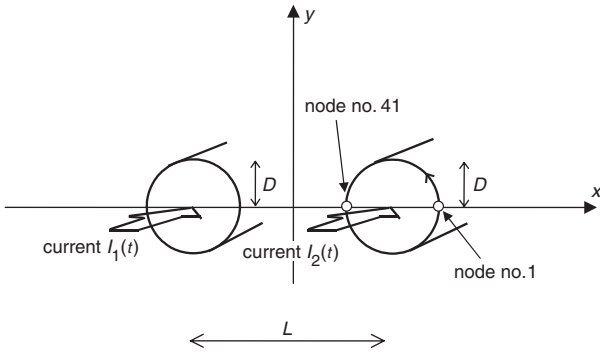

Fig. 1 *Simulation set-up*

Under these conditions the electromagnetic field distribution in both regions can be described by the following equations

a. Conducting domain

$$\begin{aligned} &\nabla\times\vec{E} = -\mu_1\partial\vec{H}/\partial t;\\ &\nabla\times\vec{H} = \sigma\vec{E}; \qquad \nabla\cdot\vec{H} = 0; \qquad \nabla\cdot\vec{E} = 0 \end{aligned} \tag{7a}$$

b. Non-conducting domain

$$\begin{aligned} &\nabla\times\vec{E} = -\mu_0\partial\vec{H}/\partial t;\\ &\nabla\times\vec{H} = 0; \qquad \nabla\cdot\vec{H} = 0; \qquad \nabla\cdot\vec{E} = 0 \end{aligned} \tag{7b}$$

Because, in general, this is a three-dimensional problem it is natural to solve in terms of the scalar potential formalism. To provide uniqueness of the solution, the magnetic scalar potential ϕ in the non-conducting domain is introduced:

$$\vec{H} = \vec{H}_{fil} - \nabla\phi \tag{8}$$

$$\vec{H}_{fil} = \sum_{i=1}^{N} \left(\vec{H}_{fil}\right)_i \tag{9}$$

Here $(\vec{H}_{fil})_i$ is the magnetic field generated by an equivalent filamentary conductor carrying the current I_i. The field $(\vec{H}_{fil})_i$ can be calculated using the Biot-Savart law:

$$\begin{aligned} (\vec{H}_{fil}\ (\vec{r},t))_i &= \frac{1}{4\pi}\int_{L_i}\vec{I}_i(\vec{r}\,',t)\times\frac{\vec{r}-\vec{r}\,'}{|\vec{r}-\vec{r}\,'|^3}dl\\ &= \frac{\tilde{\theta}_0(t)}{4\pi}\int_{L_i}\vec{I}_i^{sp}(\vec{r}\,')\times\frac{\vec{r}-\vec{r}\,'}{|\vec{r}-\vec{r}\,'|^3}dl = (\vec{H}_{fil}^{sp}(\vec{r}))_i\tilde{\theta}_0(t) \end{aligned} \tag{10}$$

Substituting (8) into the third equation in (7b) yields the governing equation for the scalar potential:

$$\Delta\phi = 0 \tag{11}$$

The representation (9) and (10) not only ensures satisfaction of the second condition in (6), but also provides explicit introduction of the source term containing the total currents in the scalar potential formulation. Presence of the source term means that only nontrivial solutions are sought.

Let the duration of the pulses be such that the electromagnetic penetration depth remains much lower than the characteristic size D of the conductor's cross-section, i.e. condition (1) is met. Thus the electromagnetic field behaviour inside the conductors can be described using the surface impedance boundary conditions (5) and the solution is sought in free space only.

3 Surface integral equation

Since the scalar potential in free space obeys the Laplace equation, the boundary integral equation method [12] yields the following surface integral equation:

$$\begin{aligned} &\frac{\phi}{2} + \sum_{i=1}^{N}\int_{S_i}\phi\frac{\partial G}{\partial\vec{n}}ds = \sum_{i=1}^{N}\int_{S_i}G\frac{\partial\phi}{\partial\vec{n}}ds,\\ &G = (4\pi|\vec{r}-\vec{r}\,'|)^{-1} \end{aligned} \tag{12}$$

Here G is the fundamental solution of Laplace's equation in free space, S_i the ith conductor's surface, assumed to be smooth, and the unit normal vector $\vec{n}$ is chosen inwards. From (8) it follows that

$$\frac{\partial\phi}{\partial\vec{n}} = \vec{n}\cdot\left(\vec{H}_{fil} - \vec{H}\right) \tag{13}$$

Substituting (13) into (12) gives

$$\frac{\phi}{2} + \sum_{i=1}^{N}\int_{S_i}\phi\frac{\partial G}{\partial\vec{n}}ds = \sum_{i=1}^{N}\int_{S_i}G\vec{n}\cdot\left(\vec{H}_{fil} - \vec{H}\right)ds \tag{14}$$

Equation (14) includes two unknowns and it must be supplemented by another equation relating the functions

ϕ and $\vec{n}\cdot\vec{H}$, namely the surface impedance boundary condition (5b). Substitution of (5b) into (14) results in the following formulation

$$\frac{\phi}{2}+\sum_{i=1}^{N}\int_{S_i}\left\{\phi\frac{\partial G}{\partial\vec{n}}-G(L_1[\nabla\phi]+L_2[\nabla\phi]+L_3[\nabla\phi])\right\}ds$$
$$=\sum_{i=1}^{N}\int_{S_i}G\big(\vec{n}\cdot\vec{H}_{fil}-L_1\big[\vec{H}_{fil}\big]+L_2\big[\vec{H}_{fil}\big]+L_3\big[\vec{H}_{fil}\big]\big)ds \tag{15}$$

where

$$L_1\left[\vec{f}\right]=T_1*\sum_{i=1}^{2}\frac{\partial f_{\xi_i}}{\partial\xi_i} \tag{16a}$$

$$L_2\left[\vec{f}\right]=T_2*\sum_{i=1}^{2}\frac{d_{3-i}-d_i}{2d_id_{3-i}}\frac{\partial f_{\xi_i}}{\partial\xi_i} \tag{16b}$$

$$L_3\left[\vec{f}\right]=T_3*\sum_{i=1}^{2}\left\{\frac{3d_{3-i}^2-d_i^2-2d_id_{3-i}}{8d_i^2d_{3-i}^2}\frac{\partial f_{\xi_i}}{\partial\xi_i}+\frac{1}{2}\left(-\frac{\partial^2 f_{\xi_i}}{\partial\xi_{3-i}^2}+\frac{\partial^2 f_{\xi_i}}{\partial\xi_i^2}+2\frac{\partial^2 f_{\xi_{3-i}}}{\partial\xi_i\partial\xi_{3-i}}\right)\right\} \tag{16c}$$

and the surface coordinates have been introduced in functions T_m, which are given in (5).

Although the surface integral equation (15) can be solved with respect to ϕ, it has to be done at every time step, a process that renders this numerical procedure impractical. However, (15) can be transformed to the form suitable for efficient numerical implementation using the perturbation technique and taking into account some properties of the SIBCs. These properties are discussed next.

4 Properties of SIBCs

1. We assume that the function $\vec{f}(\vec{r},t)$ can be split into space and time components as follows

$$\vec{f}(\vec{r},t)=\vec{u}(\vec{r})v(t) \tag{17}$$

Then, it follows directly from (16), that the operators L_m, $m=1$, 2, 3 can be represented in the form of superposition of the space operator $\Psi_m[\vec{u}]$ and the time operator $\Omega_m[v]$:

$$L_m\left[\vec{f}\right]=\Omega_m[v]\Psi_m[\vec{u}],\quad m=1,2,3 \tag{18}$$

where

$$\Psi_1[\vec{u}]=\sum_{i=1}^{2}\frac{\partial u_{\xi_i}}{\partial\xi_i} \tag{19a}$$

$$\Psi_2[\vec{u}]=\sum_{i=1}^{2}\frac{d_{3-i}-d_i}{2d_id_{3-i}}\frac{\partial u_{\xi_i}}{\partial\xi_i} \tag{19b}$$

$$\Psi_3[\vec{u}]=\sum_{i=1}^{2}\left\{\frac{3d_{3-i}^2-d_i^2-2d_id_{3-i}}{8d_i^2d_{3-i}^2}\frac{\partial u_{\xi_i}}{\partial\xi_i}+\frac{1}{2}\left(-\frac{\partial^2 u_{\xi_i}}{\partial\xi_{3-i}^2}+\frac{\partial^2 u_{\xi_i}}{\partial\xi_i^2}+2\frac{\partial^2 u_{\xi_{3-i}}}{\partial\xi_i\partial\xi_{3-i}}\right)\right\} \tag{19c}$$

and

$$\Omega_1[v]=T_1*v;\quad \Omega_2[v]=T_2*v;\quad \Omega_3[v]=T_3*v \tag{20}$$

2. The time operators $\Omega_m[v]$ have the following property:

$$\Omega_2[v]=\Omega_1[\Omega_1[v]]\quad\text{and}\quad \Omega_3[v]=\Omega_2[\Omega_1[v]]=\Omega_1[\Omega_2[v]] \tag{21}$$

This property is easily proven in the Laplace domain where the operators in (20) take the form:

$$\bar{\Omega}_m[\bar{v}]=\bar{T}_m\bar{v},\qquad m=1,2,3 \tag{22}$$

where

$$\bar{T}_1(s)=(\sigma\mu_1)^{-1/2}s^{-1/2};\qquad \bar{T}_2(s)=(\sigma\mu_1)^{-1}s^{-1};\qquad \bar{T}_3(s)=(\sigma\mu_1)^{-3/2}s^{-3/2} \tag{23}$$

From (23) we obtain

$$\bar{T}_2=\bar{T}_1\bar{T}_1;\qquad \bar{T}_3=\bar{T}_1\bar{T}_1\bar{T}_1=\bar{T}_1\bar{T}_2 \tag{24}$$

Thus

$$\bar{\Omega}_2[\bar{v}]=\bar{T}_2v=\bar{T}_1\bar{T}_1v=\bar{T}_1\bar{\Omega}_1[\bar{v}]=\bar{\Omega}_1\big[\bar{\Omega}_1[\bar{v}]\big] \tag{25a}$$

$$\bar{\Omega}_3[\bar{v}]=\bar{T}_3v=\bar{T}_2\bar{T}_1v=\bar{T}_2\bar{\Omega}_1[\bar{v}]=\bar{\Omega}_2\big[\bar{\Omega}_1[\bar{v}]\big] \tag{25b}$$

$$\bar{\Omega}_3[\bar{v}]=\bar{T}_3v=\bar{T}_1\bar{T}_2v=\bar{T}_1\bar{\Omega}_2[\bar{v}]=\bar{\Omega}_1\big[\bar{\Omega}_2[\bar{v}]\big] \tag{25c}$$

Application of the inverse Laplace transform identities to (25) leads to (21).

5 The perturbation technique

It is natural to perform further transformations using non-dimensional variables. Switching in (8) to the non-dimensional variables in (2) and denoting the scale factor for the scalar potential as ϕ^*, gives:

$$\vec{\tilde{H}}H^*=\vec{\tilde{H}}_{fil}H^*-\frac{\phi^*}{D}\tilde{\nabla}\tilde{\phi} \tag{26}$$

Taking into account (3), ϕ^* can be expressed in terms of other scale factors as follows:

$$\phi^*=H^*D=I^*/(4\pi) \tag{27}$$

With non-dimensional variables (2), (3) and (27), the integral equation (15) takes the form:

$$\frac{\tilde{\phi}}{2}+\sum_{i=1}^{N}\int_{S_i}\left(\tilde{\phi}\frac{\partial\tilde{G}}{\partial\vec{n}}-\tilde{G}\sum_{m=1}^{3}p^m\tilde{L}_m\left[\tilde{\nabla}\tilde{\phi}\right]\right)d\tilde{s}=\sum_{i=1}^{N}\int_{S_i}\tilde{G}\left(\vec{n}\cdot\vec{\tilde{H}}_{fil}-\sum_{m=1}^{3}p^m\tilde{L}_m\left[\vec{\tilde{H}}_{fil}\right]\right)d\tilde{s} \tag{28}$$

where p is the small parameter defined in (4) and the dimensionless operators $\tilde{L}_m$ are written in the form:

$$\tilde{L}_1\left[\vec{\tilde{f}}\right]=\tilde{T}_1\tilde{*}\sum_{i=1}^{2}\frac{\partial\tilde{f}_{\xi_i}}{\partial\tilde{\xi}_i} \tag{29a}$$

$$\tilde{L}_2\left[\tilde{f}\right]=\tilde{T}_2\tilde{*}\sum_{i=1}^{2}\frac{\tilde{d}_{3-i}-\tilde{d}_i}{2\tilde{d}_i\tilde{d}_{3-i}}\frac{\partial\tilde{f}_{\xi_i}}{\partial\tilde{\xi}_i} \tag{29b}$$

$$\tilde{L}_3\left[\vec{\tilde{f}}\right]=\tilde{T}_3\tilde{*}\sum_{i=1}^{2}\left\{\frac{3\tilde{d}_{3-i}^2-\tilde{d}_i^2-2\tilde{d}_i\tilde{d}_{3-i}}{8\tilde{d}_i^2\tilde{d}_{3-i}^2}\frac{\partial\tilde{f}_{\xi_i}}{\partial\tilde{\xi}_i}+\frac{1}{2}\left(-\frac{\partial^2\tilde{f}_{\xi_i}}{\partial\tilde{\xi}_{3-i}^2}+\frac{\partial^2\tilde{f}_{\xi_i}}{\partial\tilde{\xi}_i^2}+2\frac{\partial^2\tilde{f}_{\xi_{3-i}}}{\partial\tilde{\xi}_i\partial\tilde{\xi}_{3-i}}\right)\right\} \tag{29c}$$

We represent the function $\tilde{\phi}$ in the form of expansions in the small parameter p:

$$\tilde{\phi}=\sum_{m=1}^{\infty}p^m\tilde{\phi}_m \tag{30}$$

Substituting the expansions (30) into (28) and equating the coefficients of equal powers of p, the following equations for the expansion coefficients are obtained:

$$\frac{\tilde{\phi}_0}{2}+\sum_{i=1}^{N}\int_{S_i}\tilde{\phi}_0\frac{\partial\tilde{G}}{\partial\vec{n}}d\tilde{s}=\sum_{i=1}^{N}\int_{S_i}\tilde{G}\left(\vec{n}\cdot\vec{\tilde{H}}_{fil}\right)d\tilde{s} \tag{31a}$$

$$\frac{\tilde{\phi}_1}{2}+\sum_{i=1}^{N}\int_{S_i}\tilde{\phi}_1\frac{\partial\tilde{G}}{\partial\vec{n}}d\tilde{s}=-\sum_{i=1}^{N}\int_{S_i}\tilde{G}\tilde{L}_1\left[\vec{\tilde{H}}_{fil}-\tilde{\nabla}\tilde{\phi}_0\right]d\tilde{s} \tag{31b}$$

$$\begin{aligned}&\frac{\tilde{\phi}_2}{2}+\sum_{i=1}^{N}\int_{S_i}\tilde{\phi}_2\frac{\partial\tilde{G}}{\partial\vec{n}}d\tilde{s}\\&=-\sum_{i=1}^{N}\int_{S_i}\tilde{G}\left(\tilde{L}_2\left[\vec{\tilde{H}}_{fil}-\tilde{\nabla}\tilde{\phi}_0\right]+\tilde{L}_1\left[-\tilde{\nabla}\tilde{\phi}_1\right]\right)d\tilde{s}\end{aligned} \tag{31c}$$

$$\begin{aligned}&\frac{\tilde{\phi}_3}{2}+\sum_{i=1}^{N}\int_{S_i}\tilde{\phi}_3\frac{\partial\tilde{G}}{\partial\vec{n}}d\tilde{s}\\&=-\sum_{i=1}^{N}\int_{S_i}\tilde{G}\left(\tilde{L}_3\left[\vec{\tilde{H}}_{fil}-\tilde{\nabla}\tilde{\phi}_0\right]+\tilde{L}_2\left[-\tilde{\nabla}\tilde{\phi}_1\right]+\tilde{L}_1\left[-\tilde{\nabla}\tilde{\phi}_2\right]\right)d\tilde{s}\end{aligned} \tag{31d}$$

6 Separation of variables

Taking into account (6), the filamentary magnetic field in (9) and (10) can be represented as:

$$\begin{aligned}\vec{\tilde{H}}_{fil}\left(\vec{\tilde{r}},\tilde{t}\right)&=\vec{\tilde{H}}^{sp}_{fil}\left(\vec{\tilde{r}}\right)\tilde{\theta}_0(\tilde{t});\\\vec{\tilde{H}}^{sp}_{fil}&=\sum_{i=1}^{N}\int_{L_i}\vec{\tilde{I}}^{sp}_i\left(\vec{\tilde{r}}'\right)\times\frac{\vec{\tilde{r}}-\vec{\tilde{r}}'}{\left|\vec{\tilde{r}}-\vec{\tilde{r}}'\right|^3}d\tilde{l}\end{aligned} \tag{32}$$

Introducing the following non-dimensional time-dependent functions $\tilde{\theta}_m$, $m=1, 2, 3$:

$$\tilde{\theta}_m(\tilde{t})=\tilde{\Omega}_m\left[\tilde{\theta}_0(\tilde{t})\right]=\tilde{T}_m(\tilde{t})\,\tilde{*}\,\tilde{\theta}_0(\tilde{t}),\quad m=1,2,3 \tag{33}$$

and using (22) gives

$$\tilde{\theta}_2=\tilde{\Omega}_2\left[\tilde{\theta}_0\right]=\tilde{\Omega}_1\left[\tilde{\Omega}_1\left[\tilde{\theta}_0\right]\right]=\tilde{\Omega}_1\left[\tilde{\theta}_1\right] \tag{34a}$$

$$\begin{aligned}\tilde{\theta}_3=&\tilde{\Omega}_3\left[\tilde{\theta}_0\right]=\tilde{\Omega}_1\left[\tilde{\Omega}_2\left[\tilde{\theta}_0\right]\right]=\tilde{\Omega}_1\left[\tilde{\theta}_2\right]\quad\text{and}\\\tilde{\theta}_3=&\tilde{\Omega}_3\left[\tilde{\theta}_0\right]=\tilde{\Omega}_2\left[\tilde{\Omega}_1\left[\tilde{\theta}_0\right]\right]=\tilde{\Omega}_2\left[\tilde{\theta}_1\right]\end{aligned} \tag{34b}$$

We seek $\tilde{\phi}_m\left(\vec{\tilde{r}},\tilde{t}\right)$ in the form:

$$\tilde{\phi}_m\left(\vec{\tilde{r}},\tilde{t}\right)=\tilde{\phi}^{sp}_m\left(\vec{\tilde{r}}\right)\tilde{\theta}_m(\tilde{t});\qquad m=0,1,2,3 \tag{35}$$

Then the operators L_m, $m=1,2,3$ can be represented in the following form according to (18), (22) and (33), (34):

$$\begin{aligned}&\tilde{L}_1\left[\vec{\tilde{H}}_{fil}-\tilde{\nabla}\tilde{\phi}_0\right]=\tilde{\Omega}_1\left[\tilde{\theta}_0\right]\tilde{\Psi}_1\left[\vec{\tilde{H}}^{sp}_{fil}-\tilde{\nabla}\tilde{\phi}^{sp}_0\right]\\&=\tilde{\theta}_1\tilde{\Psi}_1\left[\vec{\tilde{H}}^{sp}_{fil}-\tilde{\nabla}\tilde{\phi}^{sp}_0\right]\end{aligned} \tag{36a}$$

$$\begin{aligned}&\tilde{L}_2\left[\vec{\tilde{H}}_{fil}-\tilde{\nabla}\tilde{\phi}_0\right]\\&=\tilde{\Omega}_2\left[\tilde{\theta}_0\right]\tilde{\Psi}_2\left[\vec{\tilde{H}}^{sp}_{fil}-\tilde{\nabla}\tilde{\phi}^{sp}_0\right]=\tilde{\theta}_2\tilde{\Psi}_2\left[\vec{\tilde{H}}^{sp}_{fil}-\tilde{\nabla}\tilde{\phi}^{sp}_0\right]\end{aligned} \tag{37a}$$

$$\begin{aligned}\tilde{L}_1\left[-\tilde{\nabla}\tilde{\phi}_1\right]&=\tilde{\Omega}_1\left[\tilde{\theta}_1\right]\tilde{\Psi}_1\left[-\tilde{\nabla}\tilde{\phi}^{sp}_1\right]\\&=\tilde{\theta}_2\tilde{\Psi}_1\left[-\tilde{\nabla}\tilde{\phi}^{sp}_1\right]\end{aligned} \tag{37b}$$

$$\begin{aligned}&\tilde{L}_3\left[\vec{\tilde{H}}_{fil}-\tilde{\nabla}\tilde{\phi}_0\right]=\tilde{\Omega}_3\left[\tilde{\theta}_0\right]\\&\tilde{\Psi}_3\left[\vec{\tilde{H}}^{sp}_{fil}-\tilde{\nabla}\tilde{\phi}^{sp}_0\right]=\tilde{\theta}_3\tilde{\Psi}_3\left[\vec{\tilde{H}}^{sp}_{fil}-\tilde{\nabla}\tilde{\phi}^{sp}_0\right]\end{aligned} \tag{38a}$$

$$\begin{aligned}\tilde{L}_2\left[-\tilde{\nabla}\tilde{\phi}_1\right]&=\tilde{\Omega}_2\left[\tilde{\theta}_1\right]\tilde{\Psi}_2\left[-\tilde{\nabla}\tilde{\phi}^{sp}_1\right]\\&=\tilde{\theta}_3\tilde{\Psi}_2\left[-\tilde{\nabla}\tilde{\phi}^{sp}_1\right]\end{aligned} \tag{38b}$$

$$\begin{aligned}\tilde{L}_1\left[-\tilde{\nabla}\tilde{\phi}_2\right]&=\tilde{\Omega}_1\left[\tilde{\theta}_2\right]\tilde{\Psi}_1\left[-\tilde{\nabla}\tilde{\phi}^{sp}_2\right]\\&=\tilde{\theta}_3\tilde{\Psi}_1\left[-\nabla\tilde{\phi}^{sp}_2\right]\end{aligned} \tag{38c}$$

where

$$\begin{aligned}\tilde{\Psi}_1\left[\vec{\tilde{u}}\right]&=\sum_{i=1}^{2}\frac{\partial\tilde{u}_{\xi_i}}{\partial\tilde{\xi}_i},\\\tilde{\Psi}_2[\tilde{u}]&=\sum_{i=1}^{2}\frac{\tilde{d}_{3-i}-\tilde{d}_i}{2\tilde{d}_i\tilde{d}_{3-i}}\frac{\partial\tilde{u}_{\xi_i}}{\partial\tilde{\xi}_i},\ \text{and}\\\tilde{\Psi}_3[\tilde{u}]&=\sum_{i=1}^{2}\left\{\frac{3\tilde{d}^2_{3-i}-\tilde{d}^2_i-2\tilde{d}_i\tilde{d}_{3-i}}{8\tilde{d}^2_i\tilde{d}^2_{3-i}}\frac{\partial\tilde{u}_{\xi_i}}{\partial\tilde{\xi}_i}\right.\\&\quad\left.+\frac{1}{2}\left(-\frac{\partial^2\tilde{u}_{\xi_i}}{\partial\tilde{\xi}^2_{3-i}}+\frac{\partial^2\tilde{u}_{\xi_i}}{\partial\tilde{\xi}^2_i}+2\frac{\partial^2\tilde{u}_{\xi_{3-i}}}{\partial\tilde{\xi}_i\partial\xi_{3-i}}\right)\right\}\end{aligned}$$

Substituting (32), (33) and (36)–(38) into (31), the following equations for the space components $\tilde{\phi}^{sp}_m$ are obtained:

$$\frac{\tilde{\phi}^{sp}_0}{2}+\sum_{i=1}^{N}\int_{S_i}\tilde{\phi}^{sp}_0\frac{\partial\tilde{G}}{\partial\vec{n}}d\tilde{s}=\sum_{i=1}^{N}\int_{S_i}\tilde{G}\left(\vec{n}\cdot\vec{\tilde{H}}^{sp}_{fil}\right)d\tilde{s} \tag{39a}$$

$$\begin{aligned}&\frac{\tilde{\phi}^{sp}_1}{2}+\sum_{i=1}^{N}\int_{S_i}\tilde{\phi}^{sp}_1\frac{\partial\tilde{G}}{\partial\vec{n}}d\tilde{s}\\&=-\sum_{i=1}^{N}\int_{S_i}\tilde{G}\tilde{\Psi}_1\left[\vec{\tilde{H}}^{sp}_{fil}-\tilde{\nabla}\tilde{\phi}^{sp}_0\right]d\tilde{s}\end{aligned} \tag{39b}$$

$$\begin{aligned}&\frac{\tilde{\phi}^{sp}_2}{2}+\sum_{i=1}^{N}\int_{S_i}\tilde{\phi}^{sp}_2\frac{\partial\tilde{G}}{\partial\vec{n}}d\tilde{s}=\\&-\sum_{i=1}^{N}\int_{S_i}\tilde{G}\left(\tilde{\Psi}_2\left[\vec{\tilde{H}}^{sp}_{fil}-\tilde{\nabla}\tilde{\phi}^{sp}_0\right]+\tilde{\Psi}_1\left[-\tilde{\nabla}\tilde{\phi}^{sp}_1\right]d\tilde{s}\right)\end{aligned} \tag{39c}$$

$$\begin{aligned}&\frac{\tilde{\phi}^{sp}_3}{2}+\sum_{i=1}^{N}\int_{S_i}\tilde{\phi}^{sp}_0\frac{\partial\tilde{G}}{\partial\vec{n}}d\tilde{s}=\\&-\sum_{i=1}^{N}\int_{S_i}\tilde{G}\left(\tilde{\Psi}_3\left[\vec{\tilde{H}}^{sp}_{fil}-\tilde{\nabla}\tilde{\phi}^{sp}_0\right]\right.\\&\left.+\tilde{\Psi}_2\left[-\tilde{\nabla}\tilde{\phi}^{sp}_1\right]+\tilde{\Psi}_1\left[-\tilde{\nabla}\tilde{\phi}^{sp}_2\right]\right)d\tilde{s}\end{aligned} \tag{39d}$$

It is easy to see that (39a) yields the solution in the perfect electrical conductor limit. The integral equations (39b)–(39d) give the corrections of the order of Leontovich's, Mitzner's and Rytov's approximations, respectively.

7 Final formulation in dimensional form

Returning to dimensional variables in (39) using the scale factors given in Table 1 gives:

$$\frac{\phi_0^{sp}}{2}+\sum_{i=1}^{N}\int_{S_i}\phi_0^{sp}\frac{\partial G}{\partial\vec{n}}ds=\sum_{i=1}^{N}\int_{S_i}G\left(\vec{n}\cdot\vec{H}_{fil}^{sp}\right)ds \quad (40a)$$

$$\frac{\phi_1^{sp}}{2}+\sum_{i=1}^{N}\int_{S_i}\phi_1^{sp}\frac{\partial G}{\partial\vec{n}}ds=\sum_{i=1}^{N}\int_{S_i}G\left(\Psi_1\left[\vec{H}_{fil}^{sp}-\nabla\phi_0^{sp}\right]\right)ds \quad (40b)$$

$$\frac{\phi_2^{sp}}{2}+\sum_{i=1}^{N}\int_{S_i}\phi_2^{sp}\frac{\partial G}{\partial\vec{n}}ds=-\sum_{i=1}^{N}\int_{S_i}G\left(\Psi_2\left[\vec{H}_{fil}^{sp}-\nabla\phi_0^{sp}\right]+\Psi_1\left[-\nabla\phi_1^{sp}\right]\right)ds \quad (40c)$$

$$\frac{\phi_3^{sp}}{2}+\sum_{i=1}^{N}\int_{S_i}\phi_3^{sp}\frac{\partial G}{\partial\vec{n}}d\tilde{s}=-\sum_{i=1}^{N}\int_{S_i}G\left(\Psi_3\left[\vec{H}_{fil}^{sp}-\nabla\phi_0^{sp}\right]+\Psi_2\left[-\nabla\phi_1^{sp}\right]+\Psi_1\left[-\nabla\phi_2^{sp}\right]\right)ds \quad (40d)$$

where the operators Ψ_m, $m=1, 2, 3$, are given in (19).

Table 1: Non-dimensional quantities and their scale factors

Non-dimensional quantity	Scale factor	Unit
$\tilde{\phi}_k^{sp},\quad k=0,1,2,3$	$(4\pi)^{-1}I^{*}D^{-k}$	Am^{-k}
$\tilde{H}_{fil}^{sp}$	$(4\pi)^{-1}I^{*}D^{-1}$	Am^{-1}
$\tilde{G}$	D^{-1}	m^{-1}
$\partial\tilde{G}/\partial\vec{n}$	D^{-2}	m^{-2}
$d\tilde{s}=d\tilde{\xi}_1 d\tilde{\xi}_2$	D^2	m^2
$\partial/\partial\tilde{\xi}_1,\partial/\partial\tilde{\xi}_2$	D^{-1}	m^{-1}
$\tilde{\Psi}_k[\,],\ k=1,2,3$	D^{-k}	m^{-k}
$\tilde{T}_k,\ k=1,2,3$	$(\sigma\mu_0)^{-k/2}\tau^{(k-1)/2}=p^k\tau^{-1}D^k$	$m^k s^{-1}$
$d\tilde{t}$ (in time convolution product)	τ	s

Thus, the procedure for calculation of the distribution of the scalar potential over the conductor's surface, using (6) as initial data, consists of the following 3 steps:

a. Calculation of the field $\vec{H}_{fil}^{sp}$ using the formula

$$\vec{H}_{fil}^{sp}=\frac{1}{4\pi}\sum_{i=1}^{N}\int_{L_i}\vec{I}_i^{sp}(\vec{r}')\times\frac{\vec{r}-\vec{r}'}{|\vec{r}-\vec{r}'|^3}dl \quad (41)$$

b. Obtaining the space functions $\phi_m^{sp}(\vec{r})$, $m=0,1,2,3$, by solving the surface integral equations (40).

c. Obtaining the scalar potential using the formula

$$\phi=\left(\phi_0^{sp}\tilde{\theta}_0+\sum_{m=1}^{3}\phi_m^{sp}T_m*\tilde{\theta}_0\right) \quad (42)$$

where the time functions $T_m(t)$, $m=1,2,3$ are $T_1(t)=(\pi\sigma\mu_1)^{-1/2}t^{-1/2}$; $T_2(t)=U(t)/(\sigma\mu_1)$; and $T_3(t)=2(\pi\sigma^3\mu^3)^{-1/2}t^{1/2}$.

At this point it is worth re-emphasising the main advantages of the formulation developed:

1. The form of integral equations, including the right-hand side, is independent of the time dependence of the incident current and is determined solely by the geometric parameters of the given system of conductors. Therefore, by solving the integral equations for space components just once for a given system of conductors and multiplying the result by the corresponding time components one can obtain solutions for any time dependence of the incident current.

2. The integral equations for the various order approximations differ only in the form of the right hand side and can be solved by the same programmed routine; therefore new computational complications do not arise beyond those involved in solving the problem in the well-known perfect electrical conductor limit.

8 Conditions of applicability and numerical example

In the low frequency case the number of conditions restricting applicability of the surface impedance concept is reduced as compared with high frequency problems which were considered in [12, 13]. Clearly, convergence of the expansions (30) is required for validity of the formulation (40–42) and therefore condition (1) must be satisfied. Thus, the introduction of scale factors enables not only derivation of the formulation but also estimation of its applicability limits and approximation errors using the following formula [14]:

$$\varepsilon_m=\alpha^{m+1}\tau^{(m+1)/2},\quad \alpha=(\sigma\mu_1 D^2)^{-1/2},\quad m=1,2,3 \quad (43)$$

where the values of m equal to 1,2,3 denote Leontovich's, Mitzner's and Rytov's approximations, respectively.

However, the basic scale factors do not contain information about all features of the problem and the basic formula (43) is to be improved. In particular, the definition of the time scale factor as the duration of the pulse does not take into account the pulse shape. Another example is the space scale factor D. It has been introduced as the characteristic size of the conductor's surface but it ignores the proximity effect in problems involving more than one conductor. In order to investigate approximation errors, we solve the following problem.

Consider a system of two parallel copper conductors ($N=2$) of circular cross-section and of radius $D=21$ mm in which equal and oppositely directed current pulses flow from an external source (Fig. 1). The duration τ of the incident pulse has been chosen equal to 2 ms so that $p=0.25$. Let the conductors be sufficiently long so that the problem may be considered 2-dimensional in the plane of the cross-section of the conductors, far from their ends. The coordinate ξ_1 is directed along the conductors so that $d_1=\infty$, $d_2=D$ and the integral equations (40) reduce to the following form:

$$\frac{\phi_0^{sp}}{2}+\sum_{i=1}^{N}\int_{\Gamma_i}\phi_0^{sp}\frac{\partial G}{\partial\vec{n}}d\xi_2=-\sum_{i=1}^{N}\int_{\Gamma_i}G\left(\vec{n}\cdot\vec{H}_{fil}^{sp}\right)d\xi_2 \quad (44a)$$

$$\frac{\phi_1^{sp}}{2}+\sum_{i=1}^{N}\int_{\Gamma_i}\phi_1^{sp}\frac{\partial G}{\partial \vec{n}}d\xi_2 = -\sum_{i=1}^{N}\int_{\Gamma_i}G\left(\Psi_1\left[\vec{H}_{fil}^{sp}-\nabla\phi_0^{sp}\right]\right)d\xi_2 \quad (44b)$$

$$\frac{\phi_2^{sp}}{2}+\sum_{i=1}^{N}\int_{\Gamma_i}\phi_2^{sp}\frac{\partial G}{\partial \vec{n}}d\xi_2 = -\sum_{i=1}^{N}\int_{\Gamma_i}G\left(\Psi_2\left[\vec{H}_{fil}^{sp}-\nabla\phi_0^{sp}\right]+\Psi_1\left[-\nabla\phi_1^{sp}\right]\right)d\xi_2 \quad (44c)$$

$$\frac{\phi_3^{sp}}{2}+\sum_{i=1}^{N}\int_{\Gamma_i}\phi_3^{sp}\frac{\partial G}{\partial \vec{n}}d\xi_2 = -\sum_{i=1}^{N}\int_{\Gamma_i}G\left(\Psi_3\left[\vec{H}_{fil}^{sp}-\nabla\phi_0^{sp}\right]+\Psi_2\left[-\nabla\phi_1^{sp}\right]+\Psi_1\left[-\nabla\phi_2^{sp}\right]\right)d\xi_2 \quad (44d)$$

where Γ_i is the contour of the cross-section of the ith conductor and the Green function in the 2-dimensional case takes the form:

$$G=-2\pi\ln(|\vec{r}-\vec{r}'|)$$

To investigate the effect of the mutual location of the conductors on the approximation error, simulations have been performed for 3 different distances L between the centres of the conductors, namely 52.5 mm (2.5D), 63 mm (3D) and 168 mm (8D).

To investigate the effect of the pulse shape, the following pulses have been selected:

$$I_a(t)=I_0\tilde{\theta}_a(t);\quad I_b(t)=I_0\tilde{\theta}_b(t);\quad \tilde{\theta}_a=(t/\tau)^2;\quad \tilde{\theta}_b=\sqrt{t/\tau};\quad I_a(0)=I_b(0);\quad I_a(\tau)=I_b(\tau) \quad (45)$$

A total of 6 problems were solved using the formulation in (44), the boundary element formulation based on the time-dependent fundamental solution [2] without use of the SIBCs (the so-called 'original BEM') and a commercial finite element software [15]. The magnetic field distributions along the conductor surface at $t=\tau$ are shown in Figs. 2–7.

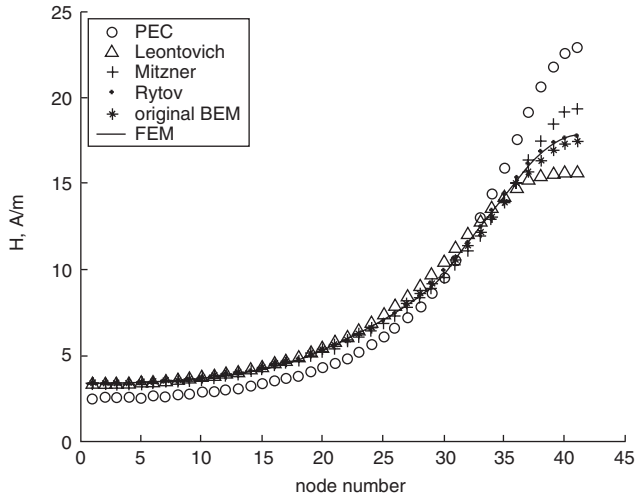

Fig. 2 *Tangential component of the magnetic field for* $I_a(t)=I_0\tilde{\theta}_a(t)$
The distance L between conductors is 52.5 mm (2.5D)

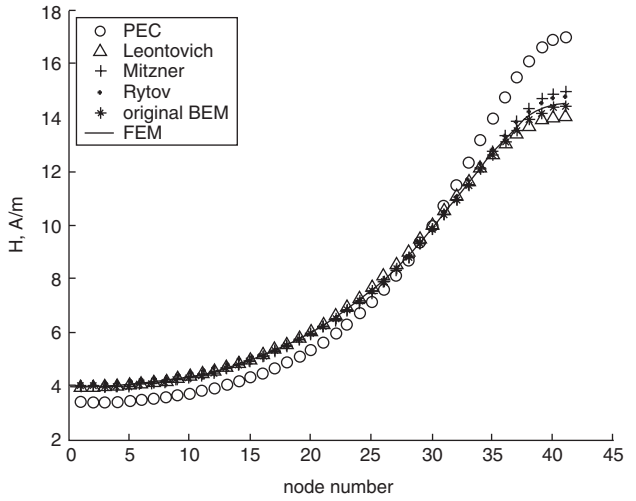

Fig. 3 *Tangential component of the magnetic field for* $I_a(t)=I_0\tilde{\theta}_a(t)$
The distance L between conductors is 63 mm (3D)

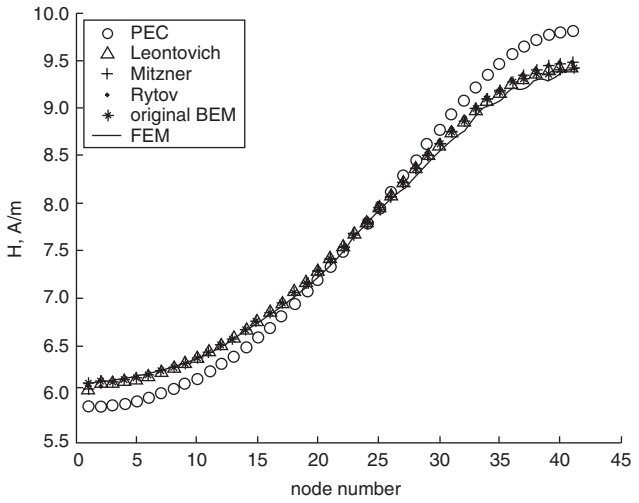

Fig. 4 *Tangential component of the magnetic field for* $I_a(t)=I_0\tilde{\theta}_a(t)$
The distance L between conductors is 168 mm (8D)

Fig. 5 *Tangential component of the magnetic field for* $I_b(t)=I_0\tilde{\theta}_b(t)$
The distance L between conductors is 52.5 mm (2.5D)

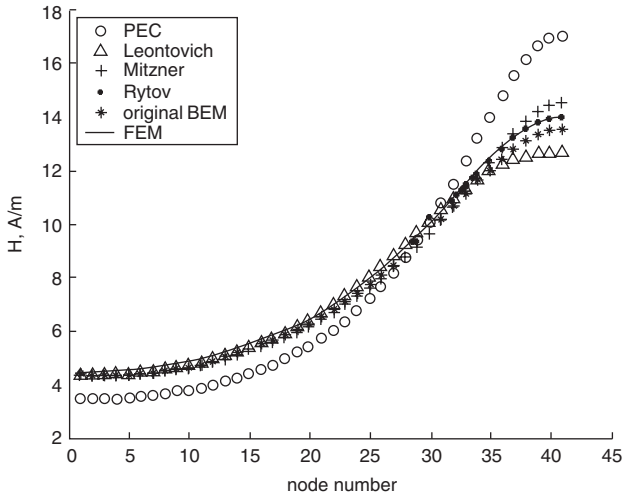

Fig. 6 *Tangential component of the magnetic field for* $I_b(t) = I_0\tilde{\theta}_b(t)$
The distance L between conductors is 63 mm ($3D$)

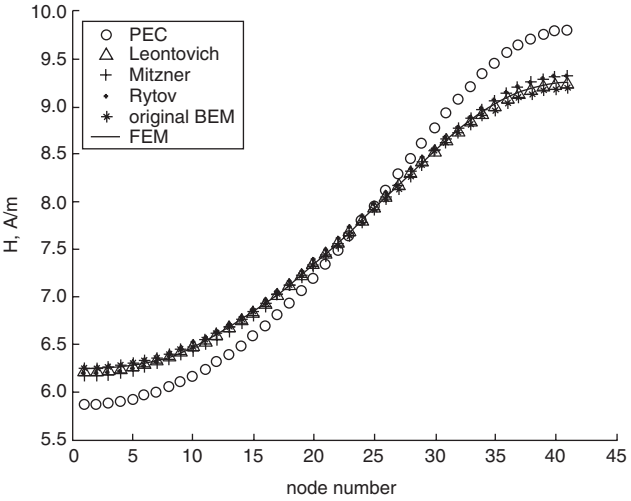

Fig. 7 *Tangential component of the magnetic field for* $I_b(t) = I_0\tilde{\theta}_b(t)$
The distance L between conductors equal to 168 mm ($8D$)

neglected in the skin effect approximation. Thus the approximation error is highest in cases of strong proximity effect. Alternatively, when the conductors are located far from each other, the effect of symmetry may be significant, especially in our case of circular cross-section. It tends to smooth out non-uniformities in the field distribution around the conductor's surface so that the surface field values are lowest in Figs. 4 and 7 resulting in a decrease in the approximation error.

Approximation errors calculated as the maximum relative error between BEM-SIBC and the 'original BEM' solutions can be seen in Table 2 together with results given by (43). The accuracy of the 'original BEM' solution is estimated to be within 1%.

As can be noted, (43) does not give a good estimation of the approximation error in cases of strong skin effect. The disagreement due to proximity effect may be reduced if we redefine the space scale factor D for the case of multi-conductor system as follows:

$$D = \min(d_{\min}, h_{\min}) \tag{46}$$

where h_{min} is shortest distance between the conductors of the system and $d_{\min}$ is the minimum radius of curvature of the surfaces of the conductors. Application of (46) to the problems shown in Figs. 2 and 5 leads to new value of D equal to 10.4 m. Under these conditions, (43) yields more accurate estimation, shown in Table 3 .

From the results shown in Figs. 2 and 3 and 4 and 5 it follows that the disagreement between curves given by the BEM-SIBC and the 'original BEM' starts earlier when the pulse I_b is used. The root of this phenomenon becomes clear if we consider the 1-dimensional problem of electromagnetic field diffusion into a conducting half-space. The distribution of the magnetic field as a function of the distance from the surface for both pulses at $t = \tau$ is shown in Fig. 8. With the pulse I_b the field penetrates deeper, and, consequently, the approximation error related to the thickness of the skin layer is higher than in the case of I_a. The increase in penetration depth causes an inductive process resulting in redistribution of the magnetic field over the surface of the conductor and in an increase in disagreement between the results obtained using the PEC limit and other approximations where the diffusion is taken into account. Therefore, if the incident pulse is such that the actual penetration depth is less than $\sqrt{\tau/(\sigma\mu_1)}$, the approximation

Table 2: Approximation errors calculated for problems shown in Figs. 2–7 and given by (43)

	$I_a(t) = I_0\tilde{\theta}_a(t)$			$I_b(t) = I_0\tilde{\theta}_b(t)$			Formula (43)
	$L = 2.5D$ (Fig. 2)	$L = 3D$ (Fig. 3)	$L = 8D$ (Fig. 4)	$L = 2.5D$ (Fig. 5)	$L = 3D$ (Fig. 6)	$L = 8D$ (Fig. 7)	
PEC	26%	17%	4%	34%	23%	6%	24.9%
Leontovich's approx.	11%	3%	$<1\%$	24%	7%	$<1\%$	6.2%
Mitzner's approx.	5%	3%	$<1\%$	7%	4%	$<1\%$	1.5%
Rytov's approx.	4%	3%	$<1\%$	5%	4%	$<1\%$	0.4%

Analysis of the results in Figs. 2–7 shows that the values of the field at the surface of the conductor are highest when the proximity effect is strongest (Figs. 2 and 5, node 41). It leads to deeper penetration of the field inside the conductor near node 41 and, consequently, to an increase in the role of the tangential derivatives that are error may be less than predicted by (43) but, at the same time, improvement of accuracy provided by the Leontovich and other approximations over the PEC limit may not be significant.

Since representation (35) enables the function $\tilde{\theta}_0$ be included explicitly in the power series (30), the role of the

Table 3: Approximation errors calculated for problems shown in Figs. 2 and 5 and given by (43) using the definition in (46)

	Fig. 2	Fig. 5	Formula (43) corrected
PEC	26%	34%	50%
Leontovich's approx.	11%	24%	25%
Mitzner's approx.	5%	7%	12%
Rytov's approx.	4%	5%	6%

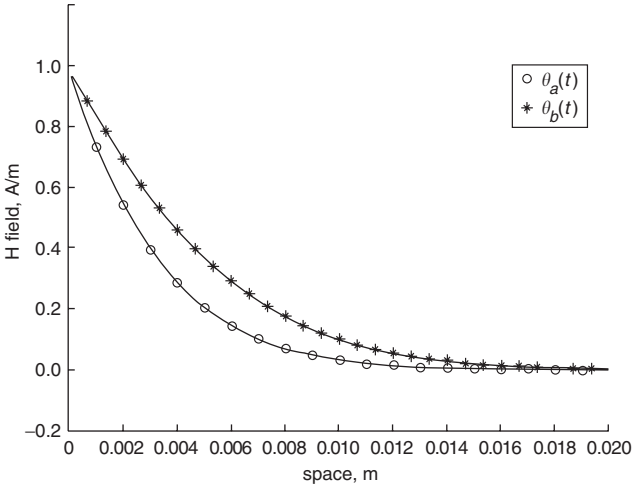

Fig. 8 *Distribution of the functions $\theta_a(t)$ and $\theta_b(t)$ inside the conductor at $t=\tau$*

pulse shape in a given problem can be estimated by analysing the functions $\tilde{\theta}_m/\tilde{\theta}_{m-1}=\left(\tilde{T}_m * \tilde{\theta}_0\right)/\left(\tilde{T}_{m-1} * \tilde{\theta}_0\right)$, $m=1,2,3$. For instance, the solution in the PEC limit would be still accurate if $p=0.2$ and $\max(\tilde{\theta}_1/\tilde{\theta}_0)=0.05$. Analysis of distributions of the functions $\tilde{\theta}_m$ shown in Fig. 8 for pulses I_a and I_b, respectively, lead to the following results: $\max(\tilde{\theta}_1/\tilde{\theta}_0)_a$=0.58; $\max(\tilde{\theta}_1/\tilde{\theta}_0)_b$=0.86; $\max(\tilde{\theta}_2/\tilde{\theta}_1)_a$= 0.59; $\max(\tilde{\theta}_2/\tilde{\theta}_1)_b=0.78$; $\max(\tilde{\theta}_3/\tilde{\theta}_2)_a=0.52$; and $\max(\tilde{\theta}_3/\tilde{\theta}_2)_b=0.67$.

Figures 9 and 10 show plots of the functions $\tilde{\theta}_m(\tilde{t})=\tilde{T}_m(\tilde{t})*\tilde{\theta}_0(\tilde{t})$for both pulses. Finally, in order to take into account the pulse shape, the following improved error formula can replace (43) (see Table 4):

$$\varepsilon_m=\alpha^{m+1}\tau^{(m+1)/2}\cdot\max(\tilde{\vartheta}_{m+1}/\tilde{\vartheta}_m) \qquad (47)$$

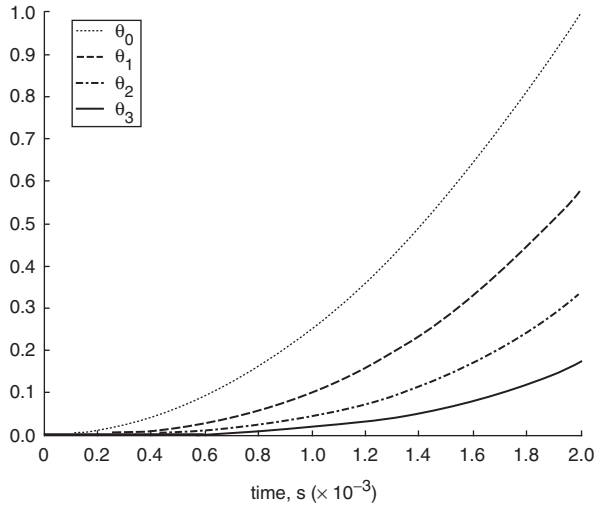

Fig. 9 *Functions $\tilde{\theta}_m$ for $I_a(t)=I_0\tilde{\theta}_a(t)$ ($\tilde{\theta}_0=\tilde{\theta}_a$ and $\tilde{\theta}_m=\tilde{\theta}_a * \tilde{T}_m$, $m=1,2,3$)*

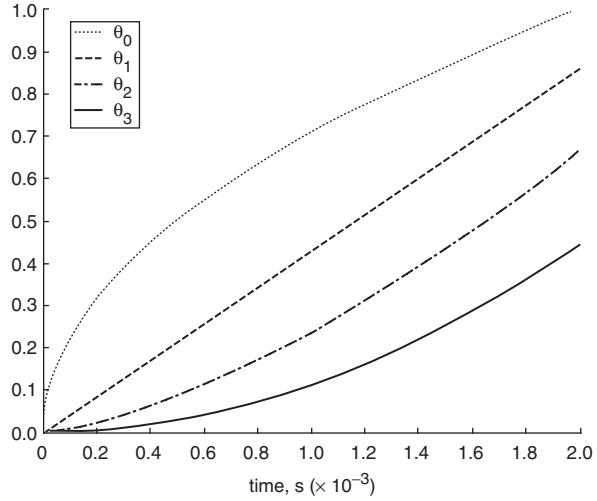

Fig. 10 *Functions $\tilde{\theta}_m$ for $I_b(t)=I_0\tilde{\theta}_b(t)$ ($\tilde{\theta}_0=\tilde{\theta}_b$ and $\tilde{\theta}_m=\tilde{\theta}_b * \tilde{T}_m$, $m=1,2,3$)*

9 Conclusions

A time domain boundary element formulation employing the surface impedance boundary conditions (SIBCs) developed in Part I of this paper was developed and applied for the computation of 3-dimensional transient fields in cylindrical conductors. Various order approximations were used to show the need and indeed the benefit of higher order SIBCs. These SIBCs were implemented in a surface integral formalism using the perturbation technique in the small parameter proportional to the ratio of the skin depth

Table 4: Approximation errors calculated for problems shown in Figs. 2–7 and given by (47)

	$I_a(t)=I_0\tilde{\theta}_a(t)$						$I_b(t)=I_0\tilde{\theta}_b(t)$					
	$L=2.5D$		$L=3D$		$L=8D$		$L=2.5D$		$L=3D$		$L=8D$	
	Error	(47)	Error	(47)	Error	(47)	Error	(47)	Error	(47)	Error	(47)
PEC	26%	29%	17%	14%	4%	14.4%	34%	42.9%	23%	21.5%	6%	21%
Leontovich	11%	14%	3%	4%	<1%	3.6%	24%	19.3%	7%	4.8%	<1%	5%
Mitzner	5%	6%	3%	0.8%	<1%	0.8%	7%	8.3%	4%	1%	<1%	1%
Rytov	4%	6%	3%	0.4%	<1%	0.4%	5%	6.2%	4%	0.4%	<1%	0.4%

and characteristic size of the conductor's surface. The formulation was tested on the problem of conductors subject to pulsed currents in the presence of skin and proximity effects. The various formulations were compared in terms of approximation errors with respect to a classical BEM solution and to FEM results, showing clear improvement in errors for the higher order solutions. Conditions of applicability of the formulation were discussed and the effect of important factors such as shape of the incident current pulse and the proximity effect were considered.

10 References

1 Yuferev, S., and Ida, N.: 'Time domain surface impedance concept for low frequency electromagnetic problems—Part I: Derivation of high order surface impedance boundary conditions in the time domain', *IEE Proc. Sci. Meas. Technol.*, 2005, **152**, (4), pp. 175–185

2 Brebbia, C.A.: 'The boundary element method for engineers' (Plymouth, London, 1980)

3 Subramaniam, S., and Hoole, S.R.: 'The impedance boundary condition in the boundary element vector potential formulation', *IEEE Trans. Magn.*, 1988, **24**, (6), pp. 2503–2505

4 Nicolas, A.: '3D eddy current solution by BIE techniques', *IEEE Trans. Magn.*, 1988, **24**, (1), pp. 130–133

5 Ahmed, M.T., Lavers, J.D., and Burke, P.E.: 'On the use of the impedance boundary condition with an indirect boundary formulation', *IEEE Trans. Magn.*, 1988, **24**, (6), pp. 2512–2514

6 Ahmed, M.T., Lavers, J.D., and Burke, P.E.: 'Direct BIE formulation for skin and proximity effect calculation with and without the use of the surface impedance approximation', *IEEE Trans. Magn.*, 1989, **25**, (4), pp. 3937–3939

7 Ishibashi, K.: 'Eddy current analysis by boundary element method utilizing impedance boundary condition', *IEEE Trans. Magn.*, 1995, **31**, (3), pp. 1500–1503

8 van Deventer, T.E., Katehi, P., and Cangellaris, A.: 'An integral equation method for the evaluation of conductor and dielectric losses in high-frequency interconnects', *IEEE Trans. Microw. Theory Tech.*, 1989, **37**, (12), pp. 1964–1972

9 Tsuboi, H., Sue, K., and Kunisue, K.: 'Surface impedance method using boundary elements for exterior regions', *IEEE Trans. Magn.*, 1991, **27**, (5), pp. 4118–4121

10 Yuferev, S., and Ida, N.: 'Selection of the surface impedance boundary conditions for a given problem', *IEEE Trans. Magn.*, 1999, **35**, (3), pp. 1486–1489

11 Hoole, S.R.H.: 'Experimental validation of the impedance boundary condition and a review of its limitations', *IEEE Trans. Magn.*, 1989, **25**, (4), pp. 3028–3030

12 Wang, D.S.: 'Limits and validity of the impedance boundary condition on penetrable surfaces', *IEEE Trans. Antennas Propag.*, 1987, **35**, (4), pp. 453–457

13 Alexopoules, N.G., and Tadler, G.A.: 'Accuracy of the Leontovich boundary condition for continuous and discontinuous surface impedance', *J. Appl. Phys.*, 1975, **46**, pp. 3326–3332

14 Barmada, S., Di Rienzo, L., Ida, N., and Yuferev, S.: 'The use of the surface impedance boundary condition in time domain problems: numerical and experimental validation', *Appl. Comput. Electromagn. Soc. J.*, 2004, **19**, (2), pp. 76–83

15 Maxwell 2D Transient, (Ansoft Corporation)